Neurobiology of Aging 34 (2013) 2239–2247

Contents lists available at SciVerse ScienceDirect

Neurobiology of Aging

journal homepage: www.elsevier.com/locate/neuaging

Critical ages in the life course of the adult brain: nonlinear subcortical aging

Anders M. Fjell [a,b,*], Lars T. Westlye [c], Håkon Grydeland [a], Inge Amlien [a], Thomas Espeseth [c,d,e], Ivar Reinvang [c], Naftali Raz [f], Dominic Holland [g], Anders M. Dale [g,h,i], Kristine B. Walhovd [a,b], the Alzheimer Disease Neuroimaging Initiative [1]

[a] Research Group for Lifespan Changes in Brain and Cognition, Department of Psychology, University of Oslo, Oslo, Norway
[b] Department of Physical Medicine and Rehabilitation, Unit of Neuropsychology, Oslo University Hospital, Oslo, Norway
[c] Department of Psychology, University of Oslo, Oslo, Norway
[d] Division for Mental Health and Addiction, Oslo University Hospital, Oslo, Norway
[e] Department of Biological and Medical Psychology, Faculty of Psychology, University of Bergen, Bergen, Norway
[f] Department of Psychology and Institute of Gerontology, Wayne State University, Detroit, MI, USA
[g] Multimodal Imaging Laboratory, University of California, San Diego, La Jolla, CA, USA
[h] Department of Radiology, University of California, San Diego, La Jolla, CA, USA
[i] Department of Neurosciences, University of California, San Diego, La Jolla, CA, USA

ARTICLE INFO

Article history:
Received 30 October 2012
Received in revised form 18 March 2013
Accepted 1 April 2013
Available online 2 May 2013

Keywords:
Aging
Magnetic resonance imaging
Longitudinal
Trajectory
Atrophy
Amygdala
Cerebral cortex
Hippocampus
Thalamus
White matter

ABSTRACT

Age-related changes in brain structure result from a complex interplay among various neurobiological processes, which may contribute to more complex trajectories than what can be described by simple linear or quadratic models. We used a nonparametric smoothing spline approach to delineate cross-sectionally estimated age trajectories of the volume of 17 neuroanatomic structures in 1100 healthy adults (18–94 years). Accelerated estimated decline in advanced age characterized some structures, for example hippocampus, but was not the norm. For most areas, 1 or 2 critical ages were identified, characterized by changes in the estimated rate of change. One-year follow-up data from 142 healthy older adults (60–91 years) confirmed the existence of estimated change from the cross-sectional analyses for all areas except 1 (caudate). The cross-sectional and the longitudinal analyses agreed well on the rank order of age effects on specific brain structures (Spearman $\rho = 0.91$). The main conclusions are that most brain structures do not follow a simple path throughout adult life and that accelerated decline in high age is not the norm of healthy brain aging.

1. Introduction

The volume of most brain structures shrinks with age, but the degree of change is highly heterogeneous across different structures (Allen et al., 2005; Raz and Rodrigue, 2006). Also, age-related changes result from a complex interplay among various neurobiological processes, which is likely to have different impact in different phases of life. This is likely to produce more complex trajectories than what can be described by linear or the usually employed higher order polynomial (quadratic or even cubic) models (Fjell et al., 2010b). The present study was undertaken with the purpose of estimating trajectories across the age of 17 brain structures in a large cross-sectional sample ($n = 1100$). Parts of these data have been previously published (e.g., Fjell et al., 2009c), and we now reanalyze them by applying a statistical approach (the smoothing spline) sensitive to local changes in estimated rate of change (Fjell et al., 2010b). This makes it possible to identify critical ages where life phases characterized by relative stability are followed by periods where estimated atrophy accelerates or critical ages where periods of estimated reduction eventually level off. The cross-sectional results were compared with longitudinal atrophy rates from a sample of 142 healthy elderly drawn from the Alzheimer's Disease Neuroimaging Initiative (ADNI) (previously presented in Fjell et al., 2009b).

* Corresponding author at: Department of Psychology, Pb. 1094 Blindern, 0317 Oslo, Norway. Tel.: +47 22 84 51 29; fax: +47 22 84 50 01.
E-mail address: andersmf@psykologi.uio.no (A.M. Fjell).

[1] Data used in the preparation of this article were obtained from the Alzheimer's Disease Neuroimaging Initiative (ADNI) database (http://www.loni.ucla.edu/ADNI). As such, the investigators within the ADNI contributed to the design and implementation of ADNI and/or provided data but did not participate in analysis or writing of this article. Complete listing of ADNI investigators is available at http://www.loni.ucla.edu/ADNI/Collaboration/ADNI_Manuscript_Citations.pdf.

0197-4580/$ – see front matter © 2013 Elsevier Inc. All rights reserved.
http://dx.doi.org/10.1016/j.neurobiolaging.2013.04.006

Table 1
Sample split by decade and sex

Age (y)	Total sample, *n* (%)	Female, *n* (%)	Male, *n* (%)
<30	315 (28.6)	186 (27.5)	129 (30.4)
30.1–40.0	121 (11.0)	72 (10.7)	49 (11.6)
40.1–50.0	154 (14.0)	94 (13.9)	60 (14.2)
50.1–60.0	159 (14.5)	107 (15.8)	52 (12.3)
61.1–70.0	187 (17.0)	114 (16.9)	73 (17.2)
71.1–80.0	123 (11.2)	74 (10.9)	49 (11.6)
>80.1	41 (3.7)	29 (4.3)	12 (2.8)
Total	1100 (100)	676 (100)	424 (100)

Previous literature, including the reports based on samples overlapping the present, indicates inverse U-shaped trajectories for hippocampus, cerebral white matter (WM), cerebellum WM, and the brain stem (Allen et al., 2005; Lupien et al., 2007; Walhovd et al., 2011), whereas U and J forms have been reported for the caudate and the ventricular system (Good et al., 2001; Sullivan et al., 1995; Walhovd et al., 2011). In contrast, mainly linear trajectories have been reported for amygdala, thalamus, accumbens, and putamen (Abe et al., 2008; Alexander et al., 2006; Allen et al., 2005; Curiati et al., 2009; Greenberg et al., 2008; Gunning-Dixon et al., 1998; Jernigan et al., 2001; Nunnemann et al., 2009; Raz et al., 2003; Sullivan et al., 2004; Walhovd et al., 2011). Both linear and quadratic reductions have been found for pallidum (Abe et al., 2008; Walhovd et al., 2011). The rational for the present study was to go beyond these general trends, by more accurately delineating the trajectories for the different structures across adult life and to identify critical ages characterized by changes in estimated rate of atrophy. We included volume for 17 major regions and structures estimated from the whole-brain segmentation approach in FreeSurfer (Fischl et al., 2002). Surface-based cortical thickness results were presented in a previous publication (Fjell et al., in press).

2. Materials and methods

2.1. Samples

2.1.1. Cross-sectional sample

A total of 1100 healthy adults (424 men and 676 women), with an age range of 76 years (18–94 years, mean = 48, standard deviation = 20) were included, pooled from 5 independent studies. Distribution of participants across decades is shown in Table 1. All the healthy samples were screened for diseases and history of neurologic conditions and dementia, and none of the participants showed signs of cognitive dysfunction. The details of each of the subsamples are described in Supplementary Table 1, but a brief description is provided here: sample 1 (Walhovd et al., 2005), $n = 69$, age 20–88 years (mean 51.3); sample 2 (Espeseth et al., 2008), $n = 208$, 19–75 years (46.8); sample 3 is from the Open Access Series of Imaging Studies (http://www.oasis-brains.org/, Marcus et al., 2007), $n = 309$, 18–94 years (44.5); sample 4 (Raz et al., 2004), $n = 191$, 18–81 years (47.3); and sample 5 (Fjell et al., 2008; Westlye et al., 2010b), $n = 323$, 20–85 years (50.8).

2.1.2. Longitudinal sample

The longitudinal sample consisted of 142 (60–90 years, mean age = 75.6 years, 48% females) participants from the Alzheimer's Disease Neuroimaging Initiative database (http://www.loni.ucla.edu/ADNI), followed for 1 year. The raw data were obtained from the ADNI database, Principal Investigator Michael W. Weiner, VA Medical Center and University of California-San Francisco. The sample is identical to that included in a previous publication (Fjell et al., 2009a) and is included to allow direct statistical comparisons with the cross-sectional results. ADNI eligibility criteria are described at http://www.adni-info.org/scientists/ADNIGrant/ProtocolSummary.aspx.

2.2. Magnetic resonance imaging processing

All scans were obtained from 1.5-T magnets from 2 different manufacturers (Siemens, Erlangen, Germany and General Electric CO, Milwaukee, WI, USA) and from 5 different models (Siemens: Avanto, Symphony, Sonata, Vision/GE: Signa). All participants within each sample were scanned on the same scanner. For details of the sequences, please consult Fjell et al. (2009b).

Cross-sectional data were processed and analyzed with FreeSurfer 4.01 (http://surfer.nmr.mgh.harvard.edu/) (Fischl et al., 2002). A neuroanatomic label is automatically assigned to each voxel in a magnetic resonance imaging volume based on probabilistic information automatically estimated from a manually labeled training set (Fischl et al., 2002). The training set included both healthy persons in the age range 18–87 years and a group of Alzheimer's disease patients in the age range 60–87 years, and the classification technique employs a registration procedure that is robust to anatomic variability, including the ventricular enlargement typically associated with aging. The technique has previously been shown to be comparable in accuracy to manual labeling (Fischl et al., 2002, 2004). An atlas-based normalization procedure used was shown to increase the robustness and accuracy of the segmentations across scanner platforms (Han and Fischl, 2007). For samples 1, 2, 3, and 5, 2–4 magnetization-prepared rapid acquisitions with gradient echo (MPRAGEs) were averaged before preprocessing to increase signal-to-noise ratio and contrast-to-noise ratio (CNR). The following structures/areas were included in the analyses: total brain volume (TBV), cerebral cortex and WM, hippocampus, amygdale, pallidum, caudate, putamen, thalamus, accumbens, brain stem, cerebellum cortex and WM, lateral ventricles, inferior lateral ventricles, and third and fourth ventricles. All segmentations were manually inspected for accuracy by an experienced operator and corrected in case of errors. Minor manual edits were performed on most participants (>80%), usually restricted to removal of nonbrain tissue, typically dura/vessels adjacent to the cortex. Additionally, presence of local artifacts sometimes caused small parts of WM to be segmented as gray matter. Such errors were routinely corrected. For 21 participants, the final segmentations were judged to be of insufficient quality, and these were thus excluded from all analyses, reducing the sample from an initial 1121 to the reported 1100.

Intracranial volume (ICV) was estimated by the use of an atlas-based normalization procedure, where the atlas scaling factor is used as a proxy for ICV, shown to correlate highly with manually derived ICV ($r = 0.93$) (Buckner et al., 2004). In previous publications with an overlapping sample pool, the results for the pooled samples were replicable in each of the subsamples (Fjell et al., 2009b; Walhovd et al., 2011), indicating that the sensitivity of detecting effects are upheld and the statistical power are increased manifold. Thus, we are convinced that the approach of pooling data from different samples yields valid results. To remove any offset effects of scanner, all analyses were done on the residuals after scanner was regressed out (see Section 2.3).

Longitudinal change was calculated by the use of Quarc, previously demonstrated to be highly sensitive to longitudinal volumetric changes based on magnetic resonance imaging (Holland and Dale, 2011; Holland et al., 2012). Two MPRAGEs at each time point were averaged to increase the signal-to-noise and contrast-to-noise ratio. An increase in signal-to-noise ratio/CNR is expected to yield more accurate change estimates. Labeling was done as described in Fischl et al. (2002) with FreeSurfer 3.0.2.

2.3. Statistical analyses

To reduce the number of comparisons, mean values for left and right hemispheres were used in all region-of-interest (ROI) analyses. Analyses were performed on residuals after the effects of sample/scanner and ICV were removed. ICV was regressed out to remove the effects of the slight age differences in head size ($r = -0.12$, $p < 10^{-n}$).

For the cross-sectional analyses, a nonparametric local smoothing model, the smoothing spline, implemented in Matlab, was fitted to the data. We have previously shown that this approach gives less-biased solutions than the more commonly employed higher order polynomial functions (Fjell et al., 2010b) and that caution should be exerted in inferring trajectories from global-fit models, for example the quadratic model. For instance, the peaks of quadratic functions will inherently depend on the age range sampled. The quadratic function is always a parabola, which sometimes causes the model to indicate a nonmonotonous age relationship when nonlinear but monotonous trajectories are a more likely. Also, for quadratic models, the second derivative is assumed to be constant across the life span and hence the point of maximum acceleration of slope change cannot be determined.

We used an algorithm that optimizes smoothing level based on a version of Bayesian Information Criterion (BIC), that is, the smoothing level that minimizes BIC for each analysis was chosen. BIC offers a relative measure of the amount of information lost when a model is used to describe a set of data and thus describes the trade-off between bias and variance in the construction of models. BIC rewards goodness of fit but includes a penalty that is an increasing function of the number of estimated parameters. Thus, BIC attempts to find the model that best explains the data with a minimum of free parameters, that is, with a largest possible smoothing level. With no smoothing, the smoothing spline will yield an extremely good apparent fit to the data, but the model would not be generalizable (overfitting). BIC takes this into account by penalizing for loss of degrees of freedom. As BIC contains scaling constants, the absolute BIC values are irrelevant. To ease comparison of BIC between ordinary least-squares linear models and smoothing spline models, we used Δ_I, which is the difference between BIC for the model and the lowest BIC and in this case the difference between the smoothing spline model and the linear ordinary least-squares model. As a rule of thumb, $\Delta_I \leq 2$ would indicate that the 2 models are essentially indistinguishable with regard to goodness of fit, $\Delta_I \geq 4$ would indicate considerable differences between the models, and $\Delta_I \geq 10$ would indicate that the linear model has essentially no support.

We calculated the ages where the slope of the local smoothing curve changed (the second derivative), using the expression $-\frac{\mathrm{d}^2 f(\mathrm{age})}{\mathrm{d}\,\mathrm{age}^2}$. We named these age points as critical ages and identified 0, 1, or 2 critical ages for each brain structure.

There were no clear differences in age distribution across samples (see Supplementary Fig. 1). To avoid possible bias resulting from uneven age distribution across samples that could not be resolved by regressing out linear effects of sample and scanner, the main smoothing spline analyses were also run for the main structures in a subset of participants without any sample × age interaction. For each sample, an equal number of participants were chosen for each decade, before the data were pooled. This sample included 522 participants, with a perfect distribution of participants across decades and samples.

For the longitudinal analyses, annual percentage change was calculated for each ROI. These results have previously been reported (Fjell et al., 2009a) but were included to allow direct comparison with the cross-sectional results. Correspondence between longitudinal data and the smoothing spline models based on the cross-sectional data was assessed in 2 ways. First, we tested whether the structures or regions that showed increases or decreases in the full cross-sectional sample also showed longitudinal increases or decreases, respectively, in the independent ADNI sample. Second, we tested to what extent the pattern of estimated change across structures was the same in the cross-sectional and the longitudinal data. Unfortunately, the ADNI database contains only data for the latter part of the age range (60–91 years); so, comparisons with the cross-sectional results cannot be done throughout the adult life span. Because the methods used to calculate longitudinal change and to fit the cross-sectional trajectories differ in important aspects and the samples do not overlap, direct comparisons of estimations of absolute rates of atrophy between the longitudinal and cross-sectional results were not performed. Longitudinal reductions were measured as proportion of change between time points and further converted to annual percentage volume change. Brain volumes in the cross-sectional data were regressed on sample and ICV, and age reductions estimated from the cross-sectional data were measured in standard deviation decline in volume in the age range 60–90 years.

3. Results

3.1. Cross-sectional data

To compare the linear and the smoothing spline models, we calculated BIC for the relationship between each brain volume and age (Supplementary Table 2, also including the quadratic model for comparison purposes). Scatterplots illustrating the estimated trajectories are presented in Fig. 1 (structures) and Fig. 2 (ventricular system). Of the 17 tested regions, a nonlinear model represented the data best for 13 (TBV, cerebral cortex and WM, hippocampus, caudate, cerebellar WM, brain stem, pallidum, putamen, and lateral, inferior lateral, third, and fourth ventricles). The linear model showed the best fit for 4 regions (nucleus accumbens, cerebellar cortex, amygdala, and thalamus). For the putamen, BIC indicated that the smoothing spline model was marginally better than a linear model (BIC = 4.16), but deviation from linearity was minute. To test the stability of the results, a split-half analysis was performed for WM volume (Supplementary Fig. 2), yielding identical spline curves.

Inspections of the plots revealed substantial differences in estimated trajectories for the nonlinear models. Especially, there were large differences in curvature. For some structures, there was a peak or an inflection point after which the age relationship increased in strength (cerebral and cerebellar WM and hippocampus, to some degree TBV and the brain stem). For cerebral WM, a nonmonotonous, inverse U-shaped relationship was observed. For other structures, advanced age was accompanied by reduction in estimated change (caudate and all ventricular cavities, to some degree cerebral cortex and pallidum). Validation analyses in the subset of participants perfectly distributed across decades in all samples confirmed the results (Supplementary Fig. 3).

For the structures that showed deviations from linearity (except putamen), critical ages, that is, the ages where estimated atrophy started to accelerate or decelerate, were identified. For some structures, 1 critical age was identified, whereas 2 were found for others (referred to as early and late critical age, see Fig. 3). Early critical age varied greatly across structures, from 31 to 59 years, and volume-age correlations differed between the defined periods. For the regions best described by a linear fit, age correlations were as follows: amygdala $r = -0.56$, putamen $r = -0.69$, thalamus $r = -0.65$, nucleus accumbens $r = -0.70$, and cerebellum gray matter $r = -0.52$.

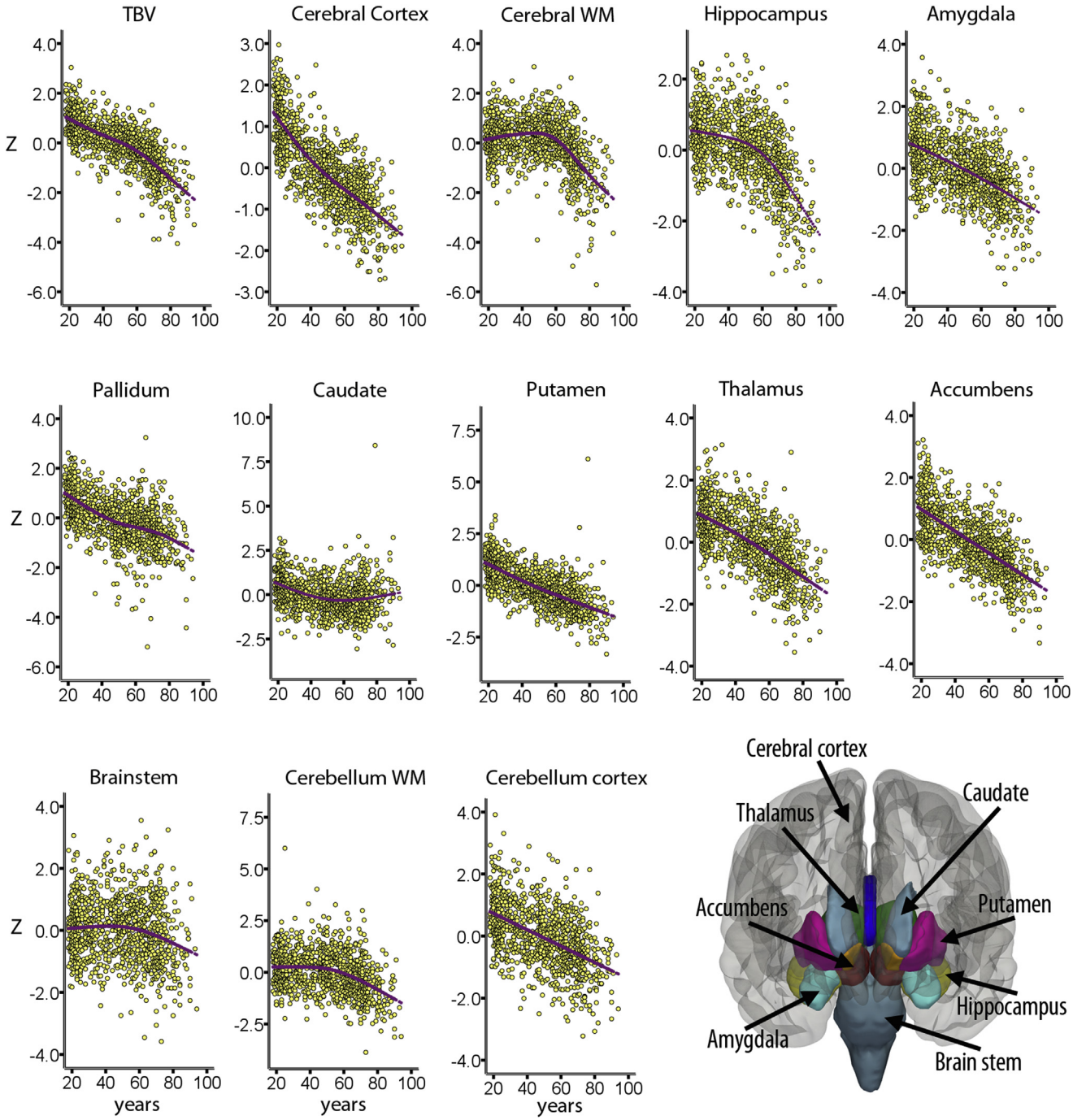

Fig. 1. Scatterplots of age-brain structure relationships. The individual data points and the cross-sectionally estimated trajectories for the 13 brain structures of interest based on the smoothing spline are shown. *Y*-axis values represent mean volume across hemispheres, corrected for the influence of sample and intracranial volume (*z* scores). The right bottom image shows some of the segmented structures of the average brain of sample 2. The 3-dimensional renderings illustrate the average shape, extension, and relative position within the brain. The cerebral cortex and underlying white matter are made transparent to allow visualization of the underlying subcortical structures. Abbreviations: TBV, total brain volume; WM, white matter.

3.2. Longitudinal validation

All ROIs showed significant longitudinal change at $p < 0.05$. This confirmed the finding of substantial atrophy/ventricular expansion observed cross-sectionally for all ROIs, except the caudate nucleus. For caudate, a weak positive correlation with age was observed after 59 years in the cross-sectional data, which was not found in the longitudinal analyses.

Next, we studied how well the pattern of cross-sectionally estimated change matched the longitudinal findings. In the age range 60–90 years, Spearman ρ between the cross-sectional estimate of shrinkage and the longitudinally measured volume loss was 0.91 ($p < 10^{-5}$). In the cross-sectional analyses, the regions with the steepest estimated decline between 60 and 90 were cerebral WM ($z = -2.20$), hippocampus ($z = -2.05$), cerebellum WM ($z = -1.29$), and thalamus ($z = -1.14$). In the longitudinal

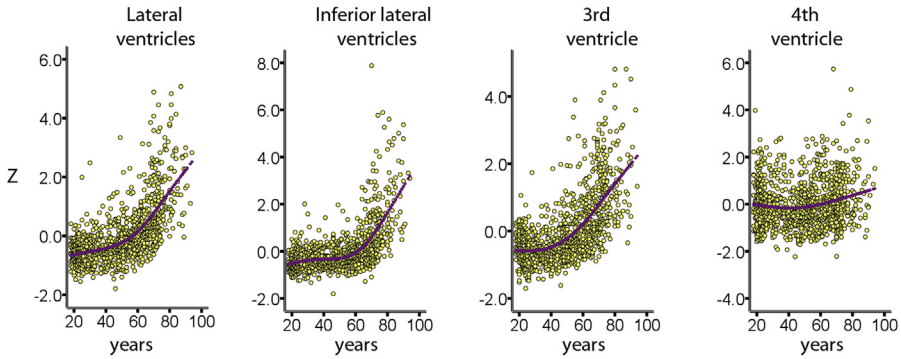

Fig. 2. Scatterplots of age-ventricular system relationships. The individual data points and the cross-sectionally estimated trajectories for the ventricles based on the smoothing spline are shown. *Y*-axis values represent mean volume across hemispheres, corrected for the influence of sample and intracranial volume (*z* scores).

analyses, the hippocampus showed the fastest shrinkage rate (−0.83% annually), followed by amygdala (−0.81%), thalamus (−0.69%), cerebral WM (−0.58%), accumbens and cerebellum WM (−0.57%), putamen (−0.43%), pallidum (−0.40%), cerebellar cortex (−0.35%), the brain stem (−0.31%), and the caudate (−0.24%). For the ventricles, there was perfect overlap between the cross-sectionally and longitudinally estimated expansion, in that the inferior lateral ventricles (cross-sectionally estimated $z = 2.92$ versus longitudinally estimated percent annual change = 5.47) showed the largest effects, followed by the lateral ventricles ($z = 2.15$ vs. 4.40%), the third ventricle ($z = 1.8$ vs. 3.07%), and the fourth ventricle ($z = 0.59$ vs. 0.71%). Thus, although there was not a one-to-one correspondence between the pattern of change across structures from the large cross-sectional sample and the longitudinal sample, there was still substantial overlap.

4. Discussion

There were 3 main findings: first, a heterogeneous pattern of discontinuous age correlations in different age spans characterized the majority of brain regions, and critical ages for changes in estimated rates of atrophy could be identified. Second, accelerated estimated reduction with advanced age is not the norm of brain aging. Rather, different structures showed a mix of trajectories. When more negative (positive for cerebrospinal fluid) age-volume correlations were seen in the last part of the age span, this would typically start in midlife. Finally, the longitudinal analyses in general supported the cross-sectional results, with a reasonably coherent pattern of atrophy across structures.

4.1. Trajectories of estimated change across the adult life span

Cross-sectional studies have shown nonlinear age relationships for the volume of several brain structures (Allen et al., 2005; Lupien et al., 2007; Raz et al., 2004), including studies with samples overlapping the present (Walhovd et al., 2011). There have, however, been few attempts to describe the trajectories in detail (for exceptions, see Fjell et al., 2010b; Jernigan et al., 2001; Schuff et al., 2012). We identified 3 basic types of trajectories:

(1) Linear reduction: amygdala, putamen, thalamus, accumbens, and the cerebellar cortex were all linearly related to age (all *r* values less than −0.52), confirming previous findings (Allen et al., 2005; Curiati et al., 2009; Gunning-Dixon et al., 1998; Jernigan et al., 2001; Walhovd et al., 2011).
(2) Stability followed by decline: hippocampus, the brain stem, and cerebellar WM exhibited initial weak age correlations but with acceleration of estimated decline from around midlife. Hippocampus is especially important because of its role in memory and early Alzheimer's disease (AD) (de Leon et al., 2006; Du et al., 2007; Fennema-Notestine et al., 2009; Jack et al., 2008; McEvoy et al., 2009). Cross-sectional studies have shown prolonged development (Ostby et al., 2009) and a marked nonlinear pattern of estimated change in adulthood (Allen et al., 2005; Fjell et al., 2010b; Jernigan and Gamst, 2005; Kennedy et al., 2009; Walhovd et al., 2005). We found that after a period of relative stability during midlife, accelerated estimated reductions started at about 50 years of age, followed by a strongly negative linear age relationship from 60 years. Cerebral WM was the only structure positively correlated with age in the earliest part of the age range, followed by a strong negative relationship. This pattern is in line with a previous publication reporting multimodal imaging data from 8 to 85 years, partly overlapping sample 5 (Westlye et al., 2010b). The ventricles showed modest estimated increase or slow decrease until 50–60 years, followed by steep estimated expansion during the last phase of life.
(3) Steep, nonlinear decline: TBV, cerebral cortex, and pallidum showed 2 critical ages with slight differences in estimated decline. TBV correlated stronger with age after 60 years than in the preceding life phases ($p < 0.05$, by use of *t* tests of Fisher *z*-transformed correlations). In contrast, pallidum and the cerebral cortex correlated stronger with age early ($p < 0.05$).

Caudate was the most deviant structure, best described by a U-shaped trajectory. We advise to interpret this with great caution, as this result was not in coherence with the longitudinal analyses and we have no reason to expect an increase in volume in the latter part of the life span.

4.2. Critical ages in estimated regional brain change

The trajectory of a neuroanatomic volume across age represents the additive combination of several neurobiological processes. We suggest that changes in the relative impact of these can be observed as turning points in the estimated change in brain volumes, what we refer to as critical ages (see Fig. 4). For instance, WM increases in volume well into adulthood (Giedd, 2004; Pfefferbaum et al., 1994; Westlye et al., 2010b; Wozniak and Lim, 2006), with myelination being 1 likely underlying factor. After midlife, volume decreases (Allen et al., 2005; Walhovd et al., 2011), likely partly caused by loss of small myelinated fibers and myelin breakdown (Meier-Ruge et al., 1992; Peters et al., 2000). This will be affected by medical conditions such as hypertension, cholesterol, diabetes, or metabolic syndrome; genetic variations such as apolipoprotein E; and

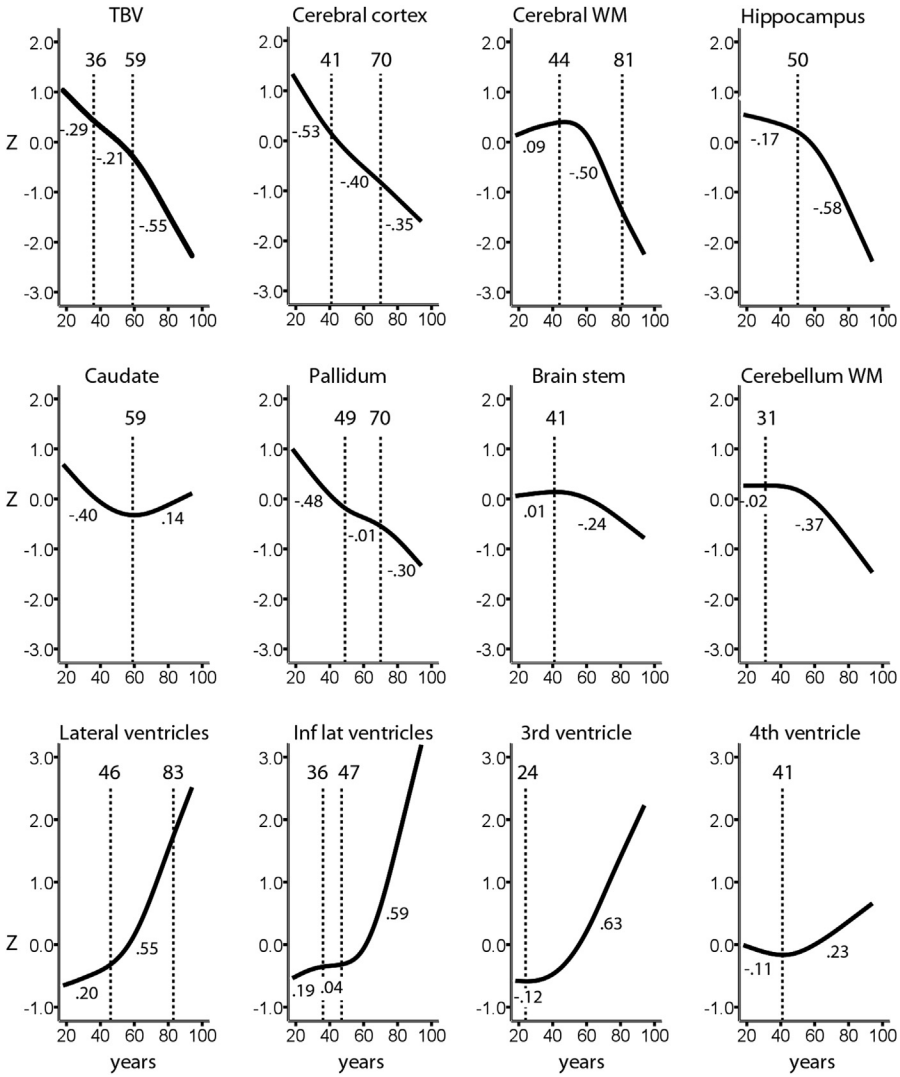

Fig. 3. Estimated age trajectories and critical ages. The estimated age trajectories from the cross-sectional analyses for the 12 areas that deviated from linearity, based on the smoothing spline, are shown. Critical ages, identified by changes in the second derivative, are displayed. Pearson correlations between brain volume and age are shown for each age phase separated by the critical ages. All correlations were significant at $p < 0.05$, except for pallidum in middle age (0.01), cerebellum white matter in young age (−0.02), and brain stem in young age (0.01). Because of small age variance, correlations are not presented for age phases defined by critical ages ≥80 years. Critical ages are indicative of phases where estimated changes in brain volumes are in transitions. Abbreviations: inf lat, inferior lateral; TBV, total brain volume; WM, white matter.

variables such as cognitive activity and education. Processes with opposite effects on WM volume probably work concurrently, for example, redundant myelination (Peters et al., 2000) and fluid bubbles in the myelin sheet with higher age (Peters and Sethares, 2002). The relative impact of each of these processes likely changes across the age span. To speculate, 1 scenario may be as follows: the additive effects of developmental processes cause the observed WM volume growth in the first half of the age span. However, after a certain age, myelin breakdown and loss of small myelinated fibers play increasingly important roles, likely before the developmental processes have come to an end. Eventually, the degenerative processes will impact the WM volume to such an extent that yearly growth is no longer linear but is gradually reduced. At this point, the second derivative of the age-volume trajectory will change, representing a critical age. As such, the estimated volume of a brain structure alone reflects the sum of many concurrent developmental and degenerative biological processes. We believe that identification of turning points may add to our understanding of the trajectories of brain volumes across the adult life span. The trajectory depicted in Fig. 4 is meant to illustrate the principle of how accumulated influence of opposing factors affects volume, but is not intended to accurately depict the life course of any single structure.

The differences in the slope of the curves between the critical ages varied greatly between structures. Whereas the cerebral cortex was almost linearly related to age, cerebral WM and the hippocampus showed large slope differences in the age ranges on each side of the critical age. Although not estimated in the present study, confidence intervals for the critical ages will likely be larger for the more linear slopes than for the distinct nonlinear and even nonmonotonous slopes.

4.3. Cross-sectional versus longitudinal results

It is impossible to infer changes in brain structures based on cross-sectional data alone (Raz and Lindenberger, 2010), as this depends on assumptions of no cohort effects and selection bias. These assumptions may generally not be valid and cross-sectional estimates of change diverge substantially (Raz et al., 2005) and sometimes even oppose longitudinal observations (Nyberg et al.,

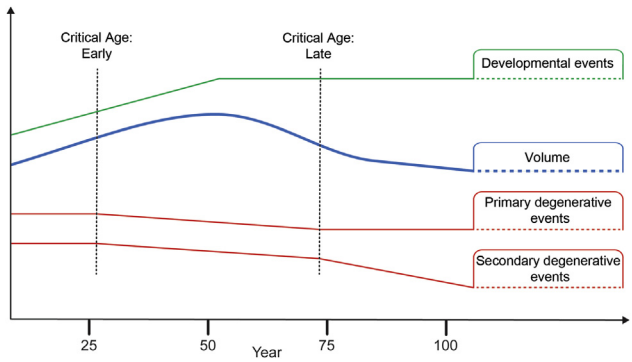

Fig. 4. A hypothetical model for discontinuous change in rate of atrophy. The figure represents a simplified attempt to visualize how 2 sets of age-dependent degenerative effects can affect the age trajectory of a brain volume and how timing of critical ages reflects the start and end point of these effects. The blue line represents the volume of a brain structure through life, for example white matter volume. In the first part of life, volume increases, caused by the sum of progressive events, for example myelination and axonal growth (green line). Before the maturational changes caused by the progressive events have come to an end, degenerative events starts, for example selective loss of small-diameter myelinated axons (primary degenerative event) and demyelination of larger connections (secondary degenerative event). The onset of these processes will affect the growth rate of the curve, detected as a change in the second derivative, and this change can be termed early critical age. After this point, the volume increase slowly decelerates. After continuous impact on the volume from these 2 processes, 1 of them eventually burns out in higher age whereas the other continues further. This causes a late critical age, where the volume reduction slowly starts to level off. This is of course a gross simplification of the processes in the brain and the trajectories that may characterize them. The main point is to illustrate that critical ages may be used in the characterization of estimated age trajectories of brain volumes and that they may be related to underlying neurobiological events, both developmental and degenerative.

2010; Raz and Lindenberger, 2011). Therefore, longitudinal data from an independent sample (Fjell et al., 2009a) were included in the present paper. With the exception of caudate volume, the direction and statistical significance of the age relationships in the cross-sectional data were confirmed by the longitudinal analyses. Further, although far from perfect, there was a reasonably coherent relationship between the pattern of atrophy between cross-sectional and longitudinal results: the structures with the largest age correlations in the cross-sectional material tended to show the highest rates of annual atrophy/ expansion. The rank-order correlation was 0.91. Thus, at least in their rank order of magnitude, the cross-sectional results for the age range >60 years seem to be largely in coherence with independent longitudinal data.

Nonetheless, caution must still be exercised in interpreting the results, as longitudinal data were available for the oldest part of the sample only. The observed correlation between age and ICV indicates that cohort differences may indeed exist in the sample. Age accounted for only 1.4% of the variance in ICV, and all analyses were performed on residuals after ICV was regressed out. As the main determinant of ICV is the lifetime maximum size of the brain, ICV corrections reduce the impact of cohort effects. Some evidence even suggests that cross-sectional studies may underestimate the extent of regional brain shrinkage in some regions (Raz et al., 2005).

Of more general concern is that the inherent problem of mapping life-span trajectories from cross-sectional examinations cannot easily be resolved with longitudinal data because longitudinal examinations of brain structures over decades are not feasible and longitudinal studies have methodological problems of their own (e.g., selective recruitment and attrition). Adding to this, most longitudinal studies are limited in age span, sample size, and number of follow-ups. To some degree, combined cross-sectional and longitudinal designs can alleviate the concerns raised above. For instance, accelerated hippocampal atrophy with age has been demonstrated (Driscoll et al., 2009; Fjell et al., 2009a; Raz et al., 2005, 2010). However, all these studies except Raz et al. (2005) comprised middle-aged and elderly participants only, and the results thus inform us less about life-span trajectories.

It is important to keep in mind that brain volumes change within relatively narrow time windows. As long as we do not know the true shape of these processes, it is unclear to know how many critical turning points are there in brain development and aging. An ideal approach to reproduce the dynamic process of change would be longitudinal studies with high density of measures and assessment of multiple time windows across the life span (Raz and Lindenberger, 2011; Raz et al., 2010).

Several factors affect the estimated trajectories at the group level and the actual trajectories at the individual level. These include genetic variations such as apolipoprotein E, and medical factors such as hypertension, cholesterol, and diabetes (for a review, see Raz et al., 2012). In addition, cognitive activity or training may impact brain structure even in older age (Zatorre et al., 2012). Future studies should further explore the impact and interactions between genetic, environmental, and medical factors on brain structure throughout the adult life. More knowledge about these processes will increase our understanding of normal brain aging. Also, possible influence of presymptomatic AD can be difficult to disentangle from normal age changes in the older participants, as follow-up examinations over several years are necessary to exclude subjects with incipient disease. However, although this factor is difficult to completely rule out from the present results, there are indications that this is not likely to have affected the trajectories to a substantial degree. Although hippocampal volume is the structure that distinguishes best between AD patients and healthy elderly, amygdala is also affected in early stages of the disease (Fjell et al., 2010a). Whereas the age slope for hippocampus is much steeper after 60 years, this is not seen for amygdala, which would be expected if incipient AD was a major factor in shaping the estimated trajectories. Even if a few of the participants had incipient AD and consequently abnormal volume decline in select structures, the smoothing spline approach is relatively robust to the influence of outliers as long as the sample size is large.

4.4. Conclusions

The present study shows that the majority of brain structures follow complex, nonlinear volumetric trajectories through adult life. Important next step to increased understanding of the mechanisms of brain aging will be to conduct large-scale, multimodal imaging studies combining, for example, volumetry, diffusion tensor imaging, and intensity/contrast measures (Fjell et al., 2008; Westlye et al., 2010a, 2010b) and also longitudinal studies with high density of measurements to examine the trajectories across age with regard to the critical phases proposed on the basis of the cross-sectional analyses.

Disclosure statement

Dr Anders M. Dale is a founder and holds equity in CorTechs Labs, Inc, and also serves on the Scientific Advisory Board. The terms of this arrangement have been reviewed and approved by the University of California, San Diego, in accordance with its conflict of interest policies.

None of the authors have any actual or potential conflicts of interest.

Acknowledgements

The present article was funded by the following grants: The Norwegian Research Council (177404 and 186092 to K.B.W., 175066

and 189507 to A.M.F., 204966 to L.T.W., 154313/V50 to I.R., 177458/V50 to T.E.), University of Oslo (to K.B.W. and A.M.F.), National Institutes of Health, USA (R37 AG011230 to N.R.), and by the European Research Council Starting Grant scheme to A.M.F and K.B.W.

The OASIS database is made available by the Washington University Alzheimer's Disease Research Center, Dr Randy Buckner at the Howard Hughes Medical Institute at Harvard University, the Neuroinformatics Research Group at Washington University School of Medicine, and the Biomedical Informatics Research Network and supported by National Institutes of Health (NIH) grants P50 AG05681, P01 AG03991, R01 AG021910, P50 MH071616, U24 RR021382, and R01 MH56584. The ADNI data collection and sharing for this project were funded by the ADNI (Principal Investigator: Michael Weiner; NIH grant U01 AG024904). ADNI is funded by the National Institute on Aging, the National Institute of Biomedical Imaging and Bioengineering, and through generous contributions from the following: Pfizer Inc, Wyeth Research, Bristol-Myers Squibb, Eli Lilly and Company, GlaxoSmithKline, Merck & Co. Inc, AstraZeneca AB, Novartis Pharmaceuticals Corporation, Alzheimer's Association, Eisai Global Clinical Development, Elan Corporation plc, Forest Laboratories, and the Institute for the Study of Aging, with participation from the US Food and Drug Administration. Industry partnerships are coordinated through the Foundation for the National Institutes of Health. The grantee organization is the Northern California Institute for Research and Education, and the study is coordinated by the Alzheimer's Disease Cooperative Study at the University of California, San Diego. ADNI data are disseminated by the Laboratory of Neuroimaging at the University of California, Los Angeles.

Appendix A. Supplementary data

Supplementary data associated with this article can be found, in the online version at http://dx.doi.org/10.1016/j.neurobiolaging.2013.04.006.

References

Abe, O., Yamasue, H., Aoki, S., Suga, M., Yamada, H., Kasai, K., Masutani, Y., Kato, N., Kato, N., Ohtomo, K., 2008. Aging in the CNS: comparison of gray/white matter volume and diffusion tensor data. Neurobiol. Aging 29, 102–116.

Alexander, G.E., Chen, K., Merkley, T.L., Reiman, E.M., Caselli, R.J., Aschenbrenner, M., Santerre-Lemmon, L., Lewis, D.J., Pietrini, P., Teipel, S.J., Hampel, H., Rapoport, S.I., Moeller, J.R., 2006. Regional network of magnetic resonance imaging gray matter volume in healthy aging. Neuroreport 17, 951–956.

Allen, J.S., Bruss, J., Brown, C.K., Damasio, H., 2005. Normal neuroanatomical variation due to age: the major lobes and a parcellation of the temporal region. Neurobiol. Aging 26, 1245–1260; discussion 1279–1282.

Buckner, R.L., Head, D., Parker, J., Fotenos, A.F., Marcus, D., Morris, J.C., Snyder, A.Z., 2004. A unified approach for morphometric and functional data analysis in young, old, and demented adults using automated atlas-based head size normalization: reliability and validation against manual measurement of total intracranial volume. Neuroimage 23, 724–738.

Curiati, P.K., Tamashiro, J.H., Squarzoni, P., Duran, F.L., Santos, L.C., Wajngarten, M., Leite, C.C., Vallada, H., Menezes, P.R., Scazufca, M., Busatto, G.F., Alves, T.C., 2009. Brain structural variability due to aging and gender in cognitively healthy elders: results from the Sao Paulo Ageing and Health study. AJNR Am. J. Neuroradiol. 30, 1850–1856.

de Leon, M.J., DeSanti, S., Zinkowski, R., Mehta, P.D., Pratico, D., Segal, S., Rusinek, H., Li, J., Tsui, W., Saint Louis, L.A., Clark, C.M., Tarshish, C., Li, Y., Lair, L., Javier, E., Rich, K., Lesbre, P., Mosconi, L., Reisberg, B., Sadowski, M., DeBernadis, J.F., Kerkman, D.J., Hampel, H., Wahlund, L.O., Davies, P., 2006. Longitudinal CSF and MRI biomarkers improve the diagnosis of mild cognitive impairment. Neurobiol. Aging 27, 394–401.

Driscoll, I., Davatzikos, C., An, Y., Wu, X., Shen, D., Kraut, M., Resnick, S.M., 2009. Longitudinal pattern of regional brain volume change differentiates normal aging from MCI. Neurology 72, 1906–1913.

Du, A.T., Schuff, N., Kramer, J.H., Rosen, H.J., Gorno-Tempini, M.L., Rankin, K., Miller, B.L., Weiner, M.W., 2007. Different regional patterns of cortical thinning in Alzheimer's disease and frontotemporal dementia. Brain 130, 1159–1166.

Espeseth, T., Westlye, L.T., Fjell, A.M., Walhovd, K.B., Rootwelt, H., Reinvang, I., 2008. Accelerated age-related cortical thinning in healthy carriers of apolipoprotein E epsilon 4. Neurobiol. Aging 29, 329–340.

Fennema-Notestine, C., Hagler Jr., D.J., McEvoy, L.K., Fleisher, A.S., Wu, E.H., Karow, D.S., Dale, A.M., 2009. Structural MRI biomarkers for preclinical and mild Alzheimer's disease. Hum. Brain Mapp. 30, 3238–3253.

Fischl, B., Salat, D.H., Busa, E., Albert, M., Dieterich, M., Haselgrove, C., van der Kouwe, A., Killiany, R., Kennedy, D., Klaveness, S., Montillo, A., Makris, N., Rosen, B., Dale, A.M., 2002. Whole brain segmentation: automated labeling of neuroanatomical structures in the human brain. Neuron 33, 341–355.

Fischl, B., Salat, D.H., van der Kouwe, A.J., Makris, N., Segonne, F., Quinn, B.T., Dale, A.M., 2004. Sequence-independent segmentation of magnetic resonance images. Neuroimage 23 (suppl 1), S69–S84.

Fjell, A.M., Walhovd, K.B., Fennema-Notestine, C., McEvoy, L.K., Hagler, D.J., Holland, D., Brewer, J.B., Dale, A.M., 2009a. One-year brain atrophy evident in healthy aging. J. Neurosci. 29, 15223–15231.

Fjell, A.M., Walhovd, K.B., Fennema-Notestine, C., McEvoy, L.K., Hagler, D.J., Holland, D., Brewer, J.B., Dale, A.M., 2010a. CSF biomarkers in prediction of cerebral and clinical change in mild cognitive impairment and Alzheimer 's disease. J. Neuroscience 10, 2088–2101.

Fjell, A.M., Walhovd, K.B., Westlye, L.T., Ostby, Y., Tamnes, C.K., Jernigan, T.L., Gamst, A., Dale, A.M., 2010b. When does brain aging accelerate? Dangers of quadratic fits in cross-sectional studies. Neuroimage 50, 1376–1383.

Fjell, A.M., Westlye, L.T., Amlien, I., Espeseth, T., Reinvang, I., Raz, N., Agartz, I., Salat, D.H., Greve, D.N., Fischl, B., Dale, A.M., Walhovd, K.B., 2009b. High consistency of regional cortical thinning in aging across multiple samples. Cereb. Cortex 19, 2001–2012.

Fjell, A.M., Westlye, L.T., Amlien, I., Espeseth, T., Reinvang, I., Raz, N., Agartz, I., Salat, D.H., Greve, D.N., Fischl, B., Dale, A.M., Walhovd, K.B., 2009c. Minute effects of sex on the aging brain: a multisample magnetic resonance imaging study of healthy aging and Alzheimer's disease. J. Neurosci. 29, 8774–8783.

Fjell, A.M., Westlye, L.T., Greve, D.N., Fischl, B., Benner, T., van der Kouwe, A.J., Salat, D., Bjørnerud, A., Due-Tønnessen, P., Walhovd, K.B., 2008. The relationship between diffusion tensor imaging and volumetry as measures of white matter properties. Neuroimage 42, 1654–1668.

Fjell, A.M., Westlye, L.T., Grydeland, H., Amlien, I., Espeseth, T., Reinvang, I., Raz, N., Dale, A.M., Walhovd, K.B., Accelerating cortical thinning: unique dementia or universal in aging? Cereb Cortex, in press.

Giedd, J.N., 2004. Structural magnetic resonance imaging of the adolescent brain. Ann. N. Y. Acad. Sci. 1021, 77–85.

Good, C.D., Johnsrude, I.S., Ashburner, J., Henson, R.N., Friston, K.J., Frackowiak, R.S., 2001. A voxel-based morphometric study of ageing in 465 normal adult human brains. Neuroimage 14, 21–36.

Greenberg, D.L., Messer, D.F., Payne, M.E., Macfall, J.R., Provenzale, J.M., Steffens, D.C., Krishnan, R.R., 2008. Aging, gender, and the elderly adult brain: an examination of analytical strategies. Neurobiol. Aging 29, 290–302.

Gunning-Dixon, F.M., Head, D., McQuain, J., Acker, J.D., Raz, N., 1998. Differential aging of the human striatum: a prospective MR imaging study. AJNR Am. J. Neuroradiol. 19, 1501–1507.

Han, X., Fischl, B., 2007. Atlas renormalization for improved brain MR image segmentation across scanner platforms. IEEE Trans. Med. Imaging 26, 479–486.

Holland, D., Dale, A.M., 2011. Nonlinear registration of longitudinal images and measurement of change in regions of interest. Med. Image Anal. 15, 489–497.

Holland, D., McEvoy, L.K., Dale, A.M., 2012. Unbiased comparison of sample size estimates from longitudinal structural measures in ADNI. Hum. Brain Mapp. 33, 2586–2602.

Jack Jr., C.R., Weigand, S.D., Shiung, M.M., Przybelski, S.A., O'Brien, P.C., Gunter, J.L., Knopman, D.S., Boeve, B.F., Smith, G.E., Petersen, R.C., 2008. Atrophy rates accelerate in amnestic mild cognitive impairment. Neurology 70, 1740–1752.

Jernigan, T.L., Archibald, S.L., Fennema-Notestine, C., Gamst, A.C., Stout, J.C., Bonner, J., Hesselink, J.R., 2001. Effects of age on tissues and regions of the cerebrum and cerebellum. Neurobiol. Aging 22, 581–594.

Jernigan, T.L., Gamst, A.C., 2005. Changes in volume with age—consistency and interpretation of observed effects. Neurobiol. Aging 26, 1271–1274; discussion 1275-1278.

Kennedy, K.M., Erickson, K.I., Rodrigue, K.M., Voss, M.W., Colcombe, S.J., Kramer, A.F., Acker, J.D., Raz, N., 2009. Age-related differences in regional brain volumes: a comparison of optimized voxel-based morphometry to manual volumetry. Neurobiol. Aging 30, 1657–1676.

Lupien, S.J., Evans, A., Lord, C., Miles, J., Pruessner, M., Pike, B., Pruessner, J.C., 2007. Hippocampal volume is as variable in young as in older adults: implications for the notion of hippocampal atrophy in humans. Neuroimage 34, 479–485.

Marcus, D.S., Wang, T.H., Parker, J., Csernansky, J.G., Morris, J.C., Buckner, R.L., 2007. Open Access Series of Imaging Studies (OASIS): cross-sectional MRI data in young, middle aged, nondemented, and demented older adults. J. Cogn. Neurosci. 19, 1498–1507.

McEvoy, L.K., Fennema-Notestine, C., Roddey, J.C., Hagler Jr., D.J., Holland, D., Karow, D.S., Pung, C.J., Brewer, J.B., Dale, A.M., Alzheimer's Disease Neuroimaging Initiative, 2009. Alzheimer disease: quantitative structural neuroimaging for detection and prediction of clinical and structural changes in mild cognitive impairment. Radiology 251, 195–205.

Meier-Ruge, W., Ulrich, J., Bruhlmann, M., Meier, E., 1992. Age-related white matter atrophy in the human brain. Ann. N. Y. Acad. Sci. 673, 260–269.

Nunnemann, S., Wohlschlager, A.M., Ilg, R., Gaser, C., Etgen, T., Conrad, B., Zimmer, C., Muhlau, M., 2009. Accelerated aging of the putamen in men but not in women. Neurobiol. Aging 30, 147–151.

Nyberg, L., Salami, A., Andersson, M., Eriksson, J., Kalpouzos, G., Kauppi, K., Lind, J., Pudas, S., Persson, J., Nilsson, L.G., 2010. Longitudinal evidence for diminished frontal cortex function in aging. Proc. Natl. Acad. Sci. U.S.A 107, 22682–22686.

Ostby, Y., Tamnes, C.K., Fjell, A.M., Westlye, L.T., Due-Tonnessen, P., Walhovd, K.B., 2009. Heterogeneity in subcortical brain development: a structural magnetic resonance imaging study of brain maturation from 8 to 30 years. J. Neurosci. 29, 11772–11782.

Peters, A., Moss, M.B., Sethares, C., 2000. Effects of aging on myelinated nerve fibers in monkey primary visual cortex. J. Comp. Neurol. 419, 364–376.

Peters, A., Sethares, C., 2002. Aging and the myelinated fibers in prefrontal cortex and corpus callosum of the monkey. J. Comp. Neurol. 442, 277–291.

Pfefferbaum, A., Mathalon, D.H., Sullivan, E.V., Rawles, J.M., Zipursky, R.B., Lim, K.O., 1994. A quantitative magnetic resonance imaging study of changes in brain morphology from infancy to late adulthood. Arch. Neurol. 51, 874–887.

Raz, N., Ghisletta, P., Rodrigue, K.M., Kennedy, K.M., Lindenberger, U., 2010. Trajectories of brain aging in middle-aged and older adults: regional and individual differences. Neuroimage 51, 501–511.

Raz, N., Gunning-Dixon, F., Head, D., Rodrigue, K.M., Williamson, A., Acker, J.D., 2004. Aging, sexual dimorphism, and hemispheric asymmetry of the cerebral cortex: replicability of regional differences in volume. Neurobiol. Aging 25, 377–396.

Raz, N., Lindenberger, U., 2010. News of cognitive cure for age-related brain shrinkage is premature: a comment on Burgmans et al. (2009). Neuropsychology 24, 255–257.

Raz, N., Lindenberger, U., 2011. Only time will tell: cross-sectional studies offer no solution to the age-brain-cognition triangle: comment on Salthouse (2011). Psychol. Bull. 137, 790–795.

Raz, N., Lindenberger, U., Rodrigue, K.M., Kennedy, K.M., Head, D., Williamson, A., Dahle, C., Gerstorf, D., Acker, J.D., 2005. Regional brain changes in aging healthy adults: general trends, individual differences and modifiers. Cereb. Cortex 15, 1676–1689.

Raz, N., Rodrigue, K.M., 2006. Differential aging of the brain: patterns, cognitive correlates and modifiers. Neurosci. Biobehav. Rev. 30, 730–748.

Raz, N., Rodrigue, K.M., Kennedy, K.M., Dahle, C., Head, D., Acker, J.D., 2003. Differential age-related changes in the regional metencephalic volumes in humans: a 5-year follow-up. Neurosci. Lett. 349, 163–166.

Raz, N., Yang, Y., Dahle, C.L., Land, S., 2012. Volume of white matter hyperintensities in healthy adults: contribution of age, vascular risk factors, and inflammation-related genetic variants. Biochim. Biophys. Acta 1822, 361–369.

Schuff, N., Tosun, D., Insel, P.S., Chiang, G.C., Truran, D., Aisen, P.S., Jack Jr., C.R., Weiner, M.W., 2012. Nonlinear time course of brain volume loss in cognitively normal and impaired elders. Neurobiol. Aging 33, 845–855.

Sullivan, E.V., Marsh, L., Mathalon, D.H., Lim, K.O., Pfefferbaum, A., 1995. Age-related decline in MRI volumes of temporal lobe gray matter but not hippocampus. Neurobiol. Aging 16, 591–606.

Sullivan, E.V., Rosenbloom, M., Serventi, K.L., Pfefferbaum, A., 2004. Effects of age and sex on volumes of the thalamus, pons, and cortex. Neurobiol. Aging 25, 185–192.

Walhovd, K.B., Fjell, A.M., Reinvang, I., Lundervold, A., Dale, A.M., Eilertsen, D.E., Quinn, B.T., Salat, D., Makris, N., Fischl, B., 2005. Effects of age on volumes of cortex, white matter and subcortical structures. Neurobiol. Aging 26, 1261–1270; discussion 1275-1268.

Walhovd, K.B., Westlye, L.T., Amlien, I., Espeseth, T., Reinvang, I., Raz, N., Agartz, I., Salat, D.H., Greve, D.N., Fischl, B., Dale, A.M., Fjell, A.M., 2011. Consistent neuroanatomical age-related volume differences across multiple samples. Neurobiol. Aging 32, 916–932.

Westlye, L.T., Walhovd, K.B., Dale, A.M., Bjornerud, A., Due-Tonnessen, P., Engvig, A., Grydeland, H., Tamnes, C.K., Ostby, Y., Fjell, A.M., 2010a. Differentiating maturational and aging-related changes of the cerebral cortex by use of thickness and signal intensity. Neuroimage 52, 172–185.

Westlye, L.T., Walhovd, K.B., Dale, A.M., Bjornerud, A., Due-Tonnessen, P., Engvig, A., Grydeland, H., Tamnes, C.K., Ostby, Y., Fjell, A.M., 2010b. Life-span changes of the human brain white matter: diffusion tensor imaging (DTI) and volumetry. Cereb. Cortex 20, 2055–2068.

Wozniak, J.R., Lim, K.O., 2006. Advances in white matter imaging: a review of in vivo magnetic resonance methodologies and their applicability to the study of development and aging. Neurosci. Biobehav. Rev. 30, 762–774.

Zatorre, R.J., Fields, R.D., Johansen-Berg, H., 2012. Plasticity in gray and white: neuroimaging changes in brain structure during learning. Nat. Neurosci. 18, 528–536.